



# Bapineuzumab captures the N-terminus of the Alzheimer's disease amyloid-beta peptide in a helical conformation

Luke A. Miles<sup>1,2,3</sup>, Gabriela A. N. Crespi<sup>1</sup>, Larissa Doughty<sup>1</sup> & Michael W. Parker<sup>1,2</sup>

<sup>1</sup>ACRF Rational Drug Discovery Centre and Biota Structural Biology Laboratory, St. Vincent's Institute of Medical Research, 9 Princes Street, Fitzroy, Victoria 3056, Australia, <sup>2</sup>Department of Biochemistry and Molecular Biology, Bio21 Molecular Science and Biotechnology Institute, University of Melbourne, Parkville, Victoria 3010, Australia, <sup>3</sup>Department of Chemical and Biomolecular Engineering, University of Melbourne, Parkville, Victoria 3010, Australia.

SUBJECT AREAS:  
NANOCRYSTALLOGRAPHY  
INTRINSICALLY DISORDERED  
PROTEINS  
ALZHEIMER'S DISEASE  
MOLECULAR NEUROSCIENCE

Received  
13 November 2012

Accepted  
4 February 2013

Published  
18 February 2013

Correspondence and requests for materials should be addressed to M.W.P. (mparker@svi.edu.au)

Bapineuzumab is a humanized antibody developed by Pfizer and Johnson & Johnson targeting the amyloid (A $\beta$ ) plaques that underlie Alzheimer's disease neuropathology. Here we report the crystal structure of a Fab-A $\beta$  peptide complex that reveals Bapineuzumab surprisingly captures A $\beta$  in a monomeric helical conformation at the N-terminus. Microscale thermophoresis suggests that the Fab binds soluble A $\beta$ (1–40) with a  $K_D$  of 89 ( $\pm$ 9) nM. The structure explains the antibody's exquisite selectivity for particular A $\beta$  species and why it cannot recognize N-terminally modified or truncated A $\beta$  peptides.

Alzheimer's disease (AD) is a common and devastating age related disease with no effective disease-modifying treatments<sup>1</sup>. Approximately, 34 million people worldwide are currently afflicted by AD and its prevalence is expected to triple over the next 40 years as people live longer<sup>2</sup>. Various antibodies targeting proteins implicated in AD are being developed as immunotherapies and are considered amongst the most promising approaches for the treatment and prevention of AD and related diseases<sup>3</sup>.

Bapineuzumab is a humanized monoclonal antibody (Mab) that targets the neurotoxic amyloid-beta (A $\beta$ ) peptide, an early biomarker of Alzheimer's disease pathology and the major component of plaques found in AD brains<sup>4</sup>. Large scale phase three clinical trials of Bapineuzumab in patients with mild to moderate Alzheimer's disease were halted in August 2012 when the drug failed to arrest cognitive decline. Despite the disappointing results, Bapineuzumab was effective in stabilizing amyloid plaque burden and lowering phosphorylated-tau levels in cerebrospinal fluid, two biomarkers of AD pathology (<http://www.alzforum.org/new/detail.asp?id=3268>). Immunotherapeutics are now being considered as prophylaxes for patients with mild cognitive impairment, many of whom go on to develop Alzheimer's disease.

The murine antibody 3D6, parent of the humanized monoclonal antibody Bapineuzumab, was raised in mice against A $\beta$  (residues 1–5) conjugated to sheep anti-mouse immunoglobulin<sup>5</sup>. Recent evidence suggests that N-terminal A $\beta$  directed antibodies interact with both soluble and insoluble forms of A $\beta$ <sup>6</sup>. Here we describe the crystal structure of the humanized antigen binding fragment (Fab) in complex with A $\beta$  (residues 1 to 28) that reveals Bapineuzumab recognizes the N-terminal end of the A $\beta$  peptide in a helical conformation. The structure provides a molecular basis for A $\beta$  recognition that may prove useful in informing the outcomes of possible future clinical trials with Bapineuzumab and other anti-AD therapeutic antibodies.

## Results

**Binding of A $\beta$ .** Amyloid- $\beta$  peptides are conformationally sensitive to their environment. DeMattos *et al.* report binding data for the parent murine intact antibody 3D6 to A $\beta$  with a  $K_D$  of  $\sim$ 5 nM to soluble and insoluble forms of A $\beta$ <sup>7</sup>. We used Microscale Thermophoresis (MST)<sup>8</sup> to measure the affinity of the humanized 3D6 antibody Fab fragment to synthetic wild type A $\beta$ <sub>40</sub>, A $\beta$ <sub>28</sub>, A $\beta$ <sub>8</sub> and N-terminally biotinylated A $\beta$ <sub>40</sub> under equivalent experimental conditions. Under these solution conditions the Fab binds wild type A $\beta$ <sub>40</sub> with a  $K_D$  of 89 ( $\pm$ 9) nM (see Supplementary Fig. S1 online), and the affinity is reduced approximately 65 fold when A $\beta$  is N-terminally biotinylated, indicating that the free N-terminus of A $\beta$  is critical for binding. Under the same solution conditions, the affinity of the Fab drops marginally to 151 ( $\pm$ 12) nM for A $\beta$ <sub>28</sub>, and quite significantly for A $\beta$ <sub>8</sub>, showing low  $\mu$ M affinity.

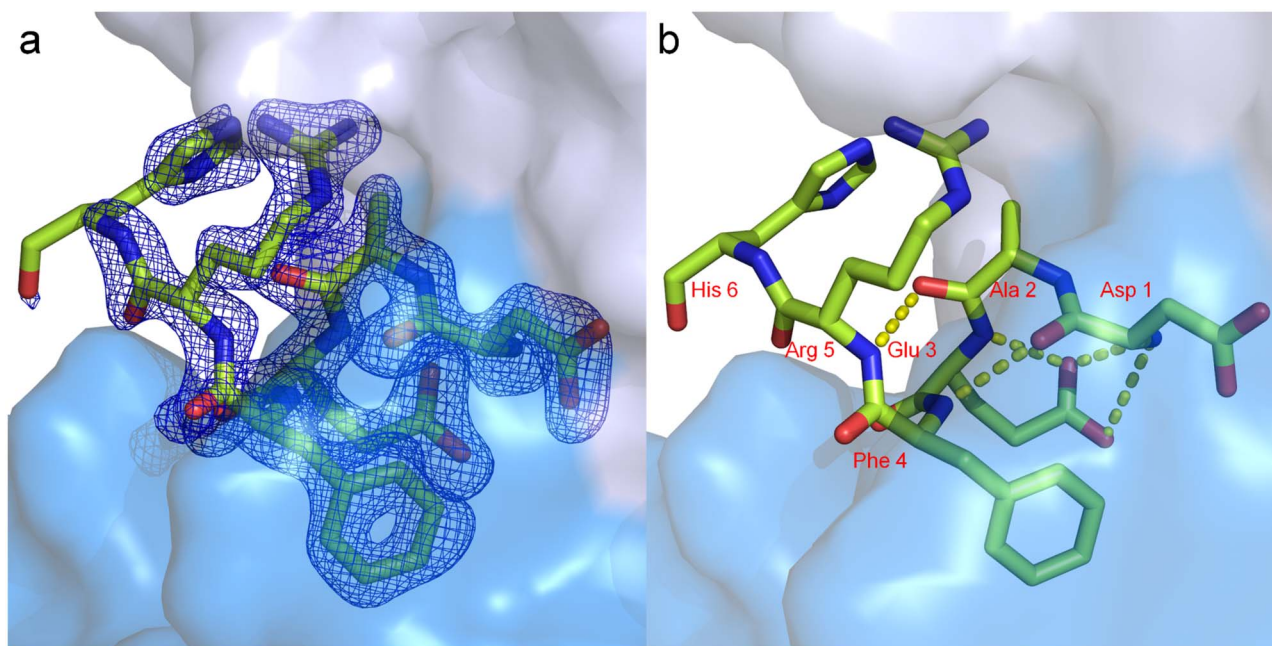


**Figure 1 | Structure of the humanized 3D6 Fab-A $\beta$  peptide complex.** Both panels show A $\beta$  nestled in the surface of the Fab CDRs. The peptide is shown in green sticks with the light chain in light blue surface and heavy chain in a darker blue surface. (a) A  $2F_o - F_c$  electron density map in the vicinity of the peptide contoured at  $1.5\sigma$ . (b) Intra-A $\beta$  hydrogen bonding, shown as dashed lines, stabilizes the helical conformation of the peptide.

We wanted to identify exactly how these N-terminal A $\beta$  (1–5) specific antibodies engage the A $\beta$  peptide. To that end we crystallized a recombinant humanized 3D6 antibody Fab fragment complexed to the A $\beta$  peptide (residues 1 to 28) and determined the complex structure to a resolution of  $2.2 \text{ \AA}$  (Fig. 1). Data refinement and model statistics are given in Table 1.

**Structure of A $\beta$ .** Fig. 1 shows the A $\beta$  peptide in the antibody binding site. We observed strong electron density across A $\beta$  residues 1–5 (DAEFR), weaker density for His 6, and no electron density for building amino acids further into the peptide sequence (Fig. 1a), presumably because they have high mobility outside the confines of the antibody. The structure shows that A $\beta$  is captured by Bapineuzumab in a helical conformation stabilized by five putative intramolecular hydrogen bonds (Fig. 1b).

Three of the five intra-A $\beta$  hydrogen bonds involve Glu 3, first between its backbone amide a side-chain carboxyl, and two bonds between the side-chain carboxyls and the free N-terminal amine of Asp 1 (Fig. 1b). Further hydrogen bonding is observed between the amide of Phe 4 and the main-chain carbonyl of Asp 1, and between the main-chain amide of Arg 5 and the carbonyl of Ala 2.

To our surprise, the A $\beta$  structure seen in the antibody complementarity determining regions (CDRs) (Fig. 2a) is very similar with TFE (2,2,2-trifluoroethylalcohol)-stabilized solution structures of A $\beta$  determined by NMR<sup>9</sup> ( $0.8 \text{ \AA}$  rms deviation on C $\alpha$  atoms when the lowest energy NMR structure is superimposed) (Fig. 2b). TFE is commonly used as a co-solvent to promote intramolecular hydrogen bonding and stabilizes secondary structure in intrinsically disordered peptides such as A $\beta$  by mimicking the solvent-deprived core of folded proteins and membranes<sup>10</sup>. Preferential binding of Bapineuzumab for plaque deposited A $\beta$ <sup>11</sup> suggests that this helical conformation at the N-terminus is either enriched or exists in an equilibrium of conformational states in dense plaque deposits. X-ray diffraction of A $\beta$  oligomers, protofibrils and fibrils suggest that the N-terminal region of the peptide is free to adopt structure independent of the core cross- $\beta$  structure<sup>12,13</sup>.

**CDR engagement of A $\beta$ .** How humanized 3D6 engages the A $\beta$  peptide is described in detail in Fig. 3. The interface surface area

between the antibody and the antigen is  $580 \text{ \AA}^2$ . Eleven possible hydrogen bonds are observed between the antibody and A $\beta$  residues Asp 1 (3 bonds), Glu 3 (4 bonds) and Arg 5 (4 bonds). In addition, there are five water-mediated hydrogen bonds. Numerous van der Waals contacts are made between antibody and A $\beta$ : nine residues from the light chain and ten residues from the heavy chain. Not surprisingly, the hydrophobic A $\beta$  residues are particularly

**Table 1 | Data collection and refinement statistics**

Data collection	
Space group	$P2_122_1$
Cell dimensions	
$a, b, c$ ( $\text{\AA}$ )	59.3, 83.0, 91.2
$\alpha, \beta, \gamma$ ( $^\circ$ )	90, 90, 90
Resolution ( $\text{\AA}$ )	2.20 (2.28–2.20) *
$R_{\text{merge}}$ (%)	16.3 (78.8)
$I/\sigma_I$	11.2 (2.8)
Completeness (%)	94.4 (75.7)
Redundancy	12.1 (5.8)
Refinement	
Resolution ( $\text{\AA}$ )	2.2
No. reflections	22098
$R_{\text{work}}/R_{\text{free}}$ (%)	17.0/22.0
No. atoms	3615
Protein	3324
Ligand/ion	54
Water	237
$B$ -factors	
Protein	20.6
Ligand/ion	19.9
Water	23.8
R.m.s. deviations	
Bond lengths ( $\text{\AA}$ )	0.005
Bond angles ( $^\circ$ )	0.98

\*Data are from a single crystal.

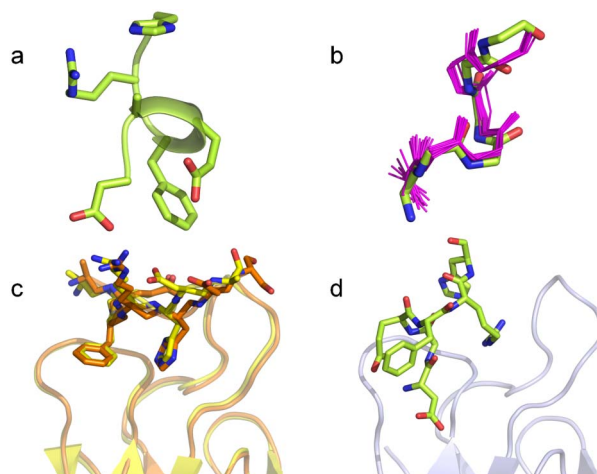


**Figure 2 | Different conformations of the A $\beta$  peptide.** (a) The helical conformational epitope of A $\beta$  recognized by Bapineuzumab highlighted in green ribbon. (b) Superposition of the main-chain heavy atoms of TFE-stabilized A $\beta$  (residues 1 to 6) NMR structures (9) (in purple) with those of A $\beta$  as recognized by Bapineuzumab (in green). (c), (d) Superposition over light chain of Fab-A $\beta$  complexes with murine antibody Fabs in (c) WO2-A $\beta$  is in orange ribbon, PFA1-A $\beta$  in yellow and (d) Bapineuzumab related Fab in grey with A $\beta$  in green sticks.

involved in van der Waals contacts: Ala 2 interacts with five residues, all from light chain CDR 3, while Phe 4 is completely enveloped by seven contacting residues (six from the heavy chain).

All hydrogen bonds stabilizing helical conformation in A $\beta$  involve the first three residues, as do most of the ligand-Fab interactions. A high proportion, perhaps 60% of A $\beta$  molecules in brain deposits are N-terminally truncated<sup>14</sup> and N-terminal truncation of A $\beta$  to any extent is likely to have deleterious effects on the stability of this helical fold and affinity for Bapineuzumab. Neurotoxic N-terminal modifications like pyro-Glu 3 (A $\beta$ <sub>pE3</sub>) found in amyloid deposits<sup>15</sup> would completely disrupt this fold and consequently presumably not be captured by Bapineuzumab. The buried free N-terminus of A $\beta$  explains the lack of cross reactivity of Bapineuzumab with the amyloid precursor protein, which is proteolytically processed to yield A $\beta$ .

#### Bapineuzumab is dissimilar to other N-terminal A $\beta$ antibodies.

This structure is unique amongst published anti-N-terminal-A $\beta$  structures. Gardberg and co-workers published the first structure of a Fab-A $\beta$  complex, murine-derived PFA1 in 2007<sup>16</sup> which was quickly followed by our own structure of a Fab derived from the murine anti-N-terminal-A $\beta$ -antibody, WO2, bound to A $\beta$ <sup>17,18</sup>. There are differences between CDR sequences of WO2 and PFA1, but they share conserved amino acids and engage the A $\beta$  N-terminal region in essentially the same way (Fig. 2c). Both report structures for A $\beta$  residues Ala 2 to Ser 8 with the core residues Phe 4, Arg 5 and His 6 buried in the CDR loops. Asp 1 is absent in each structure as are residues C-terminal to Ser 8 owing to high mobility. Contrast the two extended A $\beta$  structures shown in Fig. 2c (1.3 Å rms deviation on A $\beta$  alpha carbons upon superposition of the antibodies) with the helical A $\beta$  structure as captured by Bapineuzumab, shown in Fig. 2d.

In 2010, Basi *et al.* reported structures for the highly homologous antibodies 12A11, 10D5, and 12B4, that recognize A $\beta$  in much the same way as WO2 and PFA1/PFA2<sup>19</sup>. In contrast, Bapineuzumab CDR loops share little sequence similarity with any of these antibodies. The WWDDD motif conserved between PFA1 and PFA2, and YWDDD in WO2, is not found in the Bapineuzumab CDR-H2, where the corresponding sequence is RSGGG. Only Tyr 32 of the light chain is involved in A $\beta$  binding in all these structures. PFA1 and WO2 binding pockets have Tyr 32L pi-stacked against the aromatic

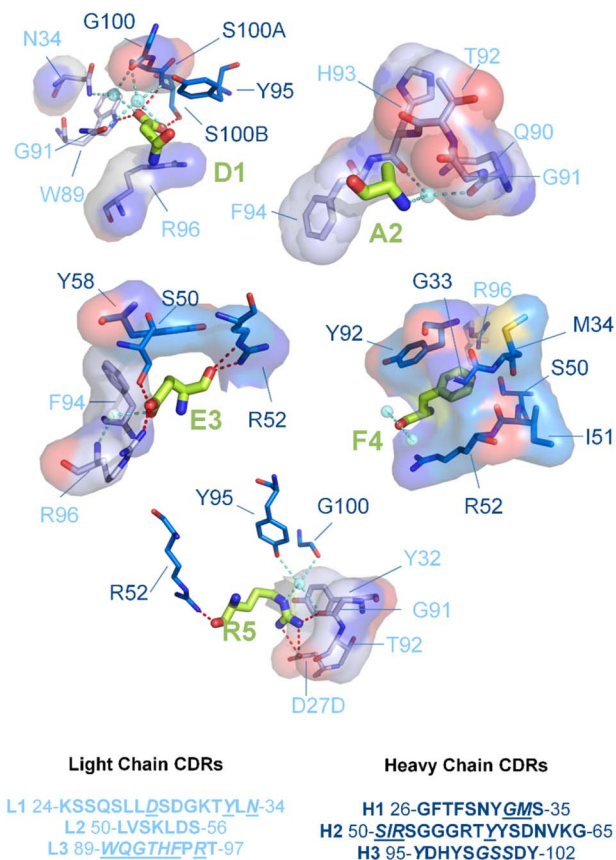


**Figure 3 | A $\beta$ -Fab interactions.** The A $\beta$  residues are shown as green sticks. Amino acid sequences corresponding to the CDRs of Bapineuzumab are shown in light blue and darker blue for light and heavy chains respectively. Amino acids involved in Fab binding to A $\beta$  are underlined and italicized in the CDR sequences common to 3D6 antibodies including Bapineuzumab. Direct polar contacts between the Fab and A $\beta$  are shown graphically as red dashed lines. Waters involved in the hydrogen bonding network are shown as aquamarine spheres, and their putative hydrogen bonds are shown as aquamarine dashed lines. Fab residue labels and carbon atoms are colored by chain (shades of blue), whereas nitrogen, oxygen and sulfur atoms are shown in dark blue, red and yellow respectively. Surfaces represent non-polar contacts to Fab residues. Intra-chain contacts have been omitted for clarity. Figure produced using LigPlus<sup>30</sup>.

side chain of His 6 in A $\beta$ . In Bapineuzumab, Tyr 32L pi-stacks against the A $\beta$  Arg 5 side-chain. The structure of the anti-AD immunotherapy Gantenerumab was reported in 2012 showing a longer extended coil structure for residues 1-11 of A $\beta$  running across the antigen binding site of the antibody, but coordinates are not available from the PDB for examination<sup>20</sup>. Given the distinct structure of A $\beta$  in Bapineuzumab and the lack of any consensus binding motif, it is clear that Bapineuzumab recognizes the overlapping binding epitope at the N-terminus in an entirely unique fashion.

#### Discussion

The recent setbacks in clinical trials of immunotherapies targeting A $\beta$  (Bapineuzumab, Solanezumab and Ponezumab) in patients with mild to moderate AD have been disappointing and expensive but very informative. In the case of Bapineuzumab, the antibody was shown to be doing what it was designed to do: promoting clearance of brain amyloid with the downstream effect of lowering phosphorylated-tau levels in the cerebrospinal fluid. And in the case of Solanezumab, there was a small but significant cognitive improvement in a cohort of patients suffering “mild” AD. Proponents of the





amyloid hypothesis of AD now believe that disease-modifying drugs may need to be administered early, in asymptomatic AD candidate patients before the disease causes its irretrievable effects<sup>21</sup> and Bapineuzumab is being considered as one of the candidates in such trials (<http://www.alzforum.org/new/detail.asp?id=3268>).

We observe a lower affinity of the humanized 3D6 antibody for A $\beta$  than the binding affinity reported by De Mattos *et al.* for the intact IgG murine antibody<sup>7</sup>. Our binding studies of truncated A $\beta$  peptides suggest a more complex picture than simple antibody recognition of a linear epitope. Our MST data suggest that the antibody does not co-opt the peptide into the helical conformation but likely binds to a population of peptide that already adopts a helical structure as seen in the crystal structure. The minimal epitope containing peptide A $\beta$ <sub>8</sub> appears to sample this helical conformation less than longer peptides under our experimental conditions. A $\beta$  peptides are highly pleiomorphic, with their conformation and oligomeric states exquisitely sensitive to their environment. Hence it was important that our measurements of the different peptides were done under the same solution conditions. An absolute  $K_D$  value can therefore be misleading, and a nuanced approach must be taken in applying these data to an *in vivo* model.

The work reported here is part of a program to determine the structural basis of how clinically relevant antibodies recognize the conformationally variable A $\beta$  peptide with the aim of aiding the interpretation of clinical trial outcomes, and for the development of more potent antibodies as elegantly demonstrated by Zahnd and co-workers where introduced mutations achieved a 500 fold improvement in antibody affinity for a helical peptide ligand<sup>22</sup>.

## Methods

Protein expression, purification and crystallization will be published in detail elsewhere (Crespi, G.A.N., Ascher, D.B., Parker, M.W. and Miles, L.A., submitted) so only a brief description is presented here.

Humanized 3D6 Fab DNA constructs (variable light chain (V<sub>L</sub>) Seq ID NO:3 and variable heavy chain (V<sub>H</sub>) Seq ID NO:4, respectively, in (23)) were synthesized and cloned into pcDNA3.1 expression plasmids (Genscript). Heavy (C-terminally hexa-histidine tagged) and light chain constructs were co-transfected into FreeStyle™ 293-F cells (Invitrogen). Cell culture supernatants were harvested by centrifugation and concentrated by tangential flow filtration (Millipore, Proflux M12). Fab was purified with Ni-NTA resin (Qiagen) followed by size exclusion chromatography, dialyzed extensively against Buffer A (20 mM HEPES pH 7.5 and 50 mM NaCl), and finally concentrated to 5 mg/mL (measured by absorbance at 280 nm) and stored in small aliquots at  $-80^{\circ}\text{C}$  until required for crystallization.

Peptides corresponding to the wild type amyloid- $\beta$  sequence (DAEFRHDSGYEVHHQKLVFFAEDVGSNKGAIIGLMVGGVV) were purchased from GenicBio (residues 1–8, 95% purity), and the corresponding 1–28 and 1–40 peptides ( $\geq 95\%$  purity) from AnaSpec. N-terminally biotinylated 1–40 peptide was a generous gift from laboratory of A/Prof. Kevin J. Barnham (Department of Pathology, the University of Melbourne). Lyophilized peptides, quantified by amino acid analysis, were resuspended in TFE and aliquoted to give 100  $\mu\text{g}$  per Eppendorf tube. All aliquots were freeze-dried for 4 hours and stored at  $-80^{\circ}\text{C}$  until required. TFE-treated, lyophilized peptides were taken up in 5  $\mu\text{L}$  of 10 mM NaOH and diluted two fold with Buffer A (20 mM HEPES pH 7.5, 50 mM NaCl) to a final concentration of 10 mg/mL. Peptide was added to Fab in a Fab:A $\beta$  molar ratio of 1:5.

Solution MST binding studies between Fab and A $\beta$  peptides (A $\beta$ <sub>40</sub>, A $\beta$ <sub>28</sub> and A $\beta$ <sub>8</sub>) were performed using standard protocols on a Monolith NT.115 (Nanotemper Technologies). Briefly, purified Fab was labeled using the RED-NHS (Amine Reactive) Protein Labelling Kit (Nanotemper Technologies). Lyophilized A $\beta$  peptide was taken up in 5  $\mu\text{L}$  of 10 mM NaOH and diluted in PBS and 0.05%v/v Tween-20. Labeled Fab antibody was mixed with A $\beta$  with a final buffer condition of PBS and 0.05% Tween-20. Each replicate contained a 16 step of 1:1 serial dilution series starting from 119  $\mu\text{M}$  of A $\beta$ <sub>40</sub>, 380  $\mu\text{M}$  of A $\beta$ <sub>8</sub> and 151  $\mu\text{M}$  of A $\beta$ <sub>28</sub>. The protein concentration was chosen such that the observed fluorescence was approximately 600 units at 50% LED power. The samples were loaded into standard capillaries and heated for 30 sec, followed by 5 sec cooling at 40% laser power for A $\beta$ <sub>40</sub> and A $\beta$ <sub>28</sub>, and 80% laser power for A $\beta$ <sub>8</sub>. All experiments were performed with a minimum of 3 independent replicates. Affinity,  $K_D$ , is quantified by analyzing the change in normalized fluorescence ( $F_{\text{norm}} = \text{fluorescence after thermophoresis}/\text{initial fluorescence}$ ) as a function of the concentration of the titrated peptide. The fraction of Fab bound ( $\Delta F_{\text{norm}}/\text{amplitude}$ ) was plotted against the concentration of peptide and the curves were analyzed using Graphpad Prism (Version 5, GraphPad, San Diego, CA, USA).

The first crystals obtained were the Fab complexed to the minimal epitope peptide A $\beta$ <sub>8</sub> with a well solution composed of 0.1 M HEPES pH 7.5, 25% (w/v) PEG 6000 (or 25% (w/v) PEG 8000). These crystals were used to promote crystallization of a

Fab:A $\beta$ <sub>28</sub> complex via microseed matrix screening<sup>24</sup>. The best crystals obtained for Fab:A $\beta$ <sub>28</sub> were grown with reservoir solution containing 0.2 M sodium formate and 20% (w/v) PEG 3350. Crystals were harvested after 2 days for diffraction studies, requiring the addition of glycerol (to 10% (v/v)) as a cryo-protectant before being flash-frozen in liquid nitrogen.

X-ray diffraction data were acquired on the MX2 beamline at the Australian Synchrotron, Clayton, Victoria, Australia. The data collection was controlled using Blue-Ice software<sup>25</sup>. Data sets of 720 images were acquired at a single wavelength of 0.9537 Å, in a nitrogen cryostream (100 K), each with 0.5° rotation per frame. The best data set was indexed, integrated and scaled in point group P222 using the HKL2000 software package<sup>26</sup>. Data collection statistics are shown in Table 1.

The initial structure was determined by molecular replacement with Phaser from the Phenix software suite<sup>27</sup> in the P2<sub>1</sub>2<sub>1</sub>2<sub>1</sub> space group. A successful molecular replacement solution was achieved with a probe model derived from an antibody Fab structure with PDB entry code 3SOB, identified in a Protein Data Bank search for sequence similarities to humanized 3D6. 10% of reflections were set aside for the free R set by the program Phenix Refine prior to the first round of refinement. Refinement and rebuilding was done with Coot<sup>28</sup> and Phenix Refine and structure validation monitored with MolProbity<sup>29</sup>. Refinement statistics are shown in Table 1. The final model has 98.0% of residues in favoured regions and 2.0% of residues in allowed regions of the Ramachandran plot with no outliers.

- Selkoe, D. J. Preventing Alzheimer's disease. *Science* **337**, 1488–1492 (2012).
- Barnes, D. E. & Yaffe, K. The projected effect of risk factor reduction on Alzheimer's disease prevalence. *Lancet Neurol.* **10**, 819–828 (2011).
- Mullard, A. Sting of Alzheimer's failures offset by upcoming prevention trials. *Nat. Rev. Drug Discov.* **11**, 657–660 (2012).
- Salloway, S. *et al.* A phase 2 multiple ascending dose trial of bapineuzumab in mild to moderate Alzheimer disease. *Neurology* **73**, 2061–2070 (2009).
- Johnson-Wood, K. *et al.* Amyloid precursor protein processing and A $\beta$ <sub>42</sub> deposition in a transgenic mouse model of Alzheimer disease. *Proc. Natl. Acad. Sci. USA.* **94**, 1550–1555 (1997).
- Zago, W. *et al.* Neutralization of soluble, synaptotoxic amyloid- $\beta$  species by antibodies is epitope specific. *J. Neurosci.* **32**, 2696–2702 (2012).
- Demattos, R. B. *et al.* A plaque-specific antibody clears existing  $\beta$ -amyloid plaques in Alzheimer's disease mice. *Neuron* **76**, 3523–3530 (2012).
- Lippok, S. *et al.* Direct detection of antibody concentration and affinity in human serum using microscale thermophoresis. *Anal. Chem.* **84**, 3523–3530 (2012).
- Zirah, S. *et al.* Structural changes of region 1–16 of the Alzheimer disease amyloid beta-peptide upon zinc binding and *in vitro* aging. *J. Biol. Chem.* **281**, 2151–2161 (2006).
- Roccatano, D., Colombo, G., Fioroni, M. & Mark, A. E. Mechanism by which 2,2,2-trifluoroethanol/water mixtures stabilize secondary-structure formation in peptides: a molecular dynamics study. *Proc. Natl. Acad. Sci. USA* **99**, 12179–12184 (2002).
- Seubert, P. *et al.* Antibody capture of soluble Abeta does not reduce cortical Abeta amyloidosis in the PDAPP mouse. *Neurodegener. Dis.* **5**, 65–71 (2008).
- Colletier, J. P. *et al.* Molecular basis for amyloid-beta polymorphism. *Proc. Natl. Acad. Sci. USA* **108**, 16938–16943 (2011).
- Stroud, J. C., Liu, C., Teng, P. K. & Eisenberg, D. Toxic fibrillar oligomers of amyloid- $\beta$  have cross- $\beta$  structure. *Proc. Natl. Acad. Sci. USA* **109**, 7717–7722 (2012).
- Sergeant, N. *et al.* Truncated beta-amyloid peptide species in pre-clinical Alzheimer's disease as new targets for the vaccination approach. *J. Neurochem.* **85**, 1581–1591 (2003).
- Nussbaum, J. M. *et al.* Prion-like behaviour and tau-dependent cytotoxicity of pyroglutamylated amyloid- $\beta$ . *Nature* **485**, 651–655 (2012).
- Gardberg, A. S. *et al.* Molecular basis for passive immunotherapy of Alzheimer's disease. *Proc. Natl. Acad. Sci. USA* **104**, 15659–15664 (2007).
- Miles, L. A. *et al.* Amyloid-beta-anti-amyloid-beta complex structure reveals an extended conformation in the immunodominant B-cell epitope. *J. Mol. Biol.* **377**, 181–192 (2008).
- Wun, K. S. *et al.* Crystallization and preliminary X-ray diffraction analysis of the Fab fragment of WO2, an antibody specific for the Abeta peptides associated with Alzheimer's disease. *Acta Crystallogr. Sect. F Struct. Biol. Cryst. Commun.* **64**, 438–441 (2008).
- Basi, G. S. *et al.* Structural correlates of antibodies associated with acute reversal of Amyloid  $\beta$ -related behavioral deficits in a mouse model of Alzheimer disease. *J. Biol. Chem.* **285**, 3417–3427 (2010).
- Bohrmann, B. *et al.* Gantenerumab: a novel human anti-A $\beta$  antibody demonstrates sustained cerebral amyloid- $\beta$  binding and elicits cell-mediated removal of human amyloid- $\beta$ . *J. Alzheimers Dis.* **28**, 49–69 (2012).
- Callaway, E. Alzheimer's drugs take a new tack. *Nature* **489**, 13–14 (2012).
- Zahnd, C., Spinelli, S., Luginbühl, B., Amstutz, P., Cambillau, C. & Plückthun, A. Directed *in vitro* evolution and crystallographic analysis of a peptide-binding single chain antibody fragment (scFv) with low picomolar affinity. *J. Biol. Chem.* **279**, 18870–18877 (2004).
- Schroeter, S. & Games, K. D. Prevention and treatment of cerebral amyloid angiopathy. US Patent Application 20080292625 (2008).



24. Obmolova, G., Malia, T. J., Teplyakov, A., Sweet, R. & Gilliland, G. L. Promoting crystallization of antibody-antigen complexes via microseed matrix screening. *Acta Crystallogr. D Biol. Crystallogr.* **66**, 927–933 (2010).
25. McPhillips, T. M. *et al.* Blu-Ice and the Distributed Control System: software for data acquisition and instrument control at macromolecular crystallography beamlines. *J. Synchrotron Radiat.* **9**, 401–406 (2002).
26. Otwinowski, Z. & Minor, W. Processing of X-ray diffraction data collected in the oscillation mode. *Methods Enzymol.* **276**, 307–326 (1997).
27. Adams, P. D. *et al.* PHENIX: a comprehensive Python-based system for macromolecular structure solution. *Acta Crystallogr. D Biol. Crystallogr.* **66**, 213–221 (2010).
28. Emsley, P., Lohkamp, B., Scott, W. G. & Cowtan, K. Features and development of Coot. *Acta Crystallogr. D Biol. Crystallogr.* **66**, 486–501 (2010).
29. Chen, V. B. *et al.* MolProbity: all-atom structure validation for macromolecular crystallography. *Acta Crystallogr. D Biol. Crystallogr.* **66**, 12–21 (2010).
30. Laskowski, R. A. & Swindells, M. B. J. LigPlot+: multiple ligand-protein interaction diagrams for drug discovery. *Chem. Inf. Model.* **51**, 2778–2786 (2011).

## Acknowledgements

We thank David Ascher for his help in developing in-house MST protocols. This research was partly undertaken on the MX1 and MX2 beamlines at the Australian Synchrotron, Victoria, Australia. This work was supported by funding from a National Health and Medical Research Council of Australia (NHMRC) Project Grant (APP1021935) and grants from the JO & JR Wicking Trust, The Mason Foundation and The Bethlehem Griffith

Research Foundation to MWP and LAM. The Australian Cancer Research Foundation provided substantial funding support for equipment critical for this work. Infrastructure support from the NHMRC Independent Research Institutes Infrastructure Support Scheme and the Victorian State Government Operational Infrastructure Support Program are gratefully acknowledged. MWP is an NHMRC Research Fellow.

## Author contributions:

G.A.N.C. expressed, purified and crystallized the Fab/Mab complexes and assisted in data acquisition. G.A.N.C. and L.D. designed and executed the MST experiments. L.A.M. acquired synchrotron diffraction data, refined data, solved structure and built model. L.A.M. and M.W.P. designed, supervised the study and analyzed the results. All authors wrote and revised the manuscript.

## Additional information

**Supplementary information** accompanies this paper at <http://www.nature.com/scientificreports>

**Competing financial interests:** The authors declare no competing financial interests.

**License:** This work is licensed under a Creative Commons Attribution-NonCommercial-NoDerivs 3.0 Unported License. To view a copy of this license, visit <http://creativecommons.org/licenses/by-nc-nd/3.0/>

**How to cite this article:** Miles, L.A., Crespi, G.A.N., Doughty, L. & Parker, M.W. Bapineuzumab captures the N-terminus of the Alzheimer's disease amyloid-beta peptide in a helical conformation. *Sci. Rep.* **3**, 1302; DOI:10.1038/srep01302 (2013).